Estimating the Ionospheric Delay Using GPS/Galileo Signals in the E5 Band

Olivier JULIEN, Lakshmi PRIYA
SIGNAV Research Group
Ecole Nationale de l'Aviation Civile (ENAC)
Toulouse, France
ojulien@recherche.enac.fr

Jean-Luc ISSLER, Laurent LESTARQUIT
Centre National d'Etudes Spatiales (CNES)
Toulouse, France
jean-luc.issler@cnes.fr, laurent.lestarquit@cnes.fr

***Abstract* — The estimation of the ionospheric delay by a GNSS receiver is quite simple when the receiver has access to signals located at different frequencies. However, when these two frequencies are very close, this estimation process becomes very noisy. The paper presents a technique to overcome this problem in the case of the reception of Galileo signals in the E5 band only. This technique is based on a local ionosphere model and the use of carrier phase dual frequency measurements. This paper also widen this investigation to the case of the reception of two GNSS constellations, GPS and Galileo, broadcasting in the same E5 band. The performance of the estimation process are shown to be very good in Europe with a standard deviation of the estimation error at L1 that is below 30cm for the worst case ionosphere conditions.**

Keywords—GNSS, Ionosphere estimation, Galileo, GPS

I. INTRODUCTION

Future Galileo and GPS open signals in Aeronautical RadioNavigation Service (ARNS) bands - E5a, E5b, E1 OS for Galileo and GPS L5, L1C - were designed so that they can bring significant improvements to most of the users compared to the current GPS L1 C/A signal performances. Receivers will thus be able to track the different signals with a lower tracking noise and a lower multipath susceptibility, and an increased resistance to interferers, consequently providing cleaner code and phase pseudorange measurements. This enhancement was obtained thanks to, among others, the use of higher code chipping rates (10.23 MHz for Galileo E5a/E5b and GPS L5), innovative modulations (ALTBOC, MBOC) and the use of a pilot channel in parallel with the traditional data channel.

The use of these open signals together can bring further obvious improvements such as (1) a more accurate and robust ionospheric delay estimation, (2) improved ambiguity resolution performances (in terms of success rate and time to fix), (3) potential tropospheric delay estimation, and (4) frequency diversity against potential intentional or unintentional jammers. These different points were backed up by many different investigations and papers from different user community needing high precision and reliable positioning, showing a great interest in a triple-frequency Galileo/GPS receiver.

Based on this triple frequency baseline, it is however important when it comes to sensitive applications, to consider degraded modes since it might impact the expected behavior of the receiver. A typical example is the loss of one frequency and it is thus important for a triple-frequency receiver to consider the loss of any of the E5a, E5b and E1 signal and its consequence on required performances.

This article specifically focuses on the event of the loss of the L1/E1 band. This situation is of particular interest because it means that the receiver is left with measurements coming exclusively from Galileo E5a/E5b and GPS L5 signals. This represents for Galileo two spectrally very close signals, and for GPS a mono-frequency case, which are not ideal cases for precise positioning. Many different figures of merit are to be investigated in this degraded mode scheme to fully assess how the receiver can cope without significantly losing any of its performance. However, this article will only focus on the ionospheric delay estimation using the available GPS/Galileo signals.

The motivation behind this investigation is to show that for a triple frequency Galileo/GPS receiver, whatever the jammed band, it is always possible to estimate accurately the ionospheric delay affecting pseudorange measurements and thus keep an interesting accuracy positioning for the receiver. Moreover, an extension of this conclusion is the potential use of the E5 band alone for precise positioning applications.

The authors have already presented initial results in 2009 [1] and 2012 [2], both using Galileo E5 signals only. These articles investigated the use of an ionospheric delay estimation process based on a Kalman Filter (KF) which was used code and carrier phase geometry free combinations, jointly with a simplified linear local model of the Vertical Total Electron Content (VTEC) to represent the ionospheric delay of any visible satellites. The initial results, based on simulations, were promising since the ionospheric delay estimation error standard deviation was at the decimeter-level for high level of solar activity assuming that the true ionosphere was perfectly modeled by the NeQuick model. This paper goes further by providing the following:

- Use of signals from two constellations in the E5 bands.
- Use of the updated NeQuick model to represent the true ionosphere, thus providing more representative results

- More extensive results in Europe based on more simulations (previous results were obtained in Sevilla, Toulouse and Stockholm during two 24h time periods representing high solar activity).

II. Description of Galileo E5 and GPS L5 signals and Associated Observable Models

A. Presentation of the Galileo E5 and GPS L5 Signals

1) Galileo E5 Signals

The Galileo E5 signals are part of the E5 band ([1164-1215 MHz] that is the largest RadioNavigation Satellite System (RNSS) band [3]. It is also an ARNS band, thus protected by ITU, but with no exclusivity to RNSS. This means that any system broadcasting within this band will have to cope with the existing non-RNSS services already present in this band. In particular, systems using strong pulsed signals, such as Distance Measuring Equipments (DME), TACtical Air Navigation (TACAN), Joint Tactical Information Distribution Systems(JTIDS)/ Multifunctional Information Distribution Systems (MIDS) are deployed in this band [4; 5].

The Galileo E5 signal has 2 components:

- The E5a signal is transmitted in the frequency band [1164 MHz – 1191.795 MHz] and centered on f_{E5a}=1176.45 MHz. It will fully support the Galileo Open Service (OS) and will support the Safety of Life (SoL) service through its ranging function. It is composed of a data and pilot channel with equal power. The data channel broadcasts the F/NAV message with a symbol rate of 50 sps. Since the useful data is encoded using a convolutional code with a constraint ½, the actual data bit rate is 25 bps. Galileo E5a is Quadra-Phase Shift Keying (QPSK)-modulated and uses a 10230-chip long spreading code with a chipping rate f_c of 10.23 Mcps. This means that it is a wide-band signal that will exhibit excellent resistance towards thermal, multipath and narrow-band interference compared to the currently available GPS C/A signal. It is also worth noting that the Galileo E5a signal will overlap the GPS L5 signal, which has similar signal characteristics. It means that it will likely be part of GPS/Galileo receivers using the E5a/L5 frequency band.
- The E5b signal is transmitted in the frequency band [1191.795 MHz – 1215 MHz], centered on f_{E5b}=1207.14 MHz. The Galileo E5b signal will support the OS, the SoL full service (ranging and integrity functions) and the Commercial Service (CS). It is composed of data and a pilot channels with equal power. The data channel broadcasts the I/NAV message (corresponding to the SoL service) with a symbol rate of 250 sps This means a useful data bit rate of 125 bps due to the convolutional encoding with a constraint 1/2. Galileo E5b uses a 10230-chip long spreading code with a chipping rate f_c of 10.23 MHz. Although the Galileo E5b does not coincide spectrally with any planned GPS signal, it has the same frequency and modulation as the future COMPASS B2 signal, which might be interoperable with Galileo E5b, and is very close to the future GLONASS L3 signal.

It can be seen that Galileo E5a and Galileo E5b are present in adjacent bands. In order to take advantage of that, the 2 signals are transmitted coherently using an ALTBOC(15,10) multiplexing [6]. The whole Galileo E5 signal is thus an extra wide-band signal (more than 50 MHz wide) that can be received:

- as a whole: this means that the user can process an extra-wide band signal for positioning, thus enjoying pseudorange measurements that are the most resistant GNSS signals towards thermal noise, multipath and narrow-band interference [7].
- separately: in this case, the user does not require a receiver with an extra-wide bandwidth, thus reducing the complexity of the receiver. Note that a dual frequency E5a/E5b receiver can process in parallel both signals, thus obtaining measurements from 2 wide-band signals that were generated based on the same satellite payload module (same filter with excellent stability over the E5 band, same HPA) at 2 different frequencies.

Compared to the Galileo E1 OS, and to a larger extend GPS L1 C/A, the Galileo E5a and E5b signals will provide enhanced tracking capabilities, and thus are very promising for precise positioning applications. Moreover, [3] specifies that both Galileo E5a and E5b signals should be received with a minimum power 2 dB above the Galileo E1 OS. This also means a better performance in case of signal obstruction.

The Galileo E5 signal performances were presented in [1] and will not be detailed in here. It is still worth mentioning that:

- the coherent code tracking performance (against thermal noise, multipath and interference) of the Galileo E5 signal is extremely good compared to any other GNSS signals due to its very wide bandwidth
- the coherent code tracking of the Galileo E5a and E5b is equivalent to that of a BPSK(10) signal.

2) GPS L5 Signal

The GPS L5 signal is transmitted in centered on $f_{L5} = f_{E5a}$=1176.45 MHz. It is composed of a data and a pilot component. It is a QPSK-modulated signal and uses 10230-chip long spreading codes with a chipping rate of 10.23 Mcps. As a consequence, it is very similar to Galileo E5a signal and exhibits very similar performance.

B. Observable Model

Let us denote $P_X^{S_Y}$ and $\varphi_X^{S_Y}$ the code and carrier phase pseudorange measurements from satellite S_Y at frequency X. Their usual model is provided by:

$$P_X^{S_Y}(k) = \begin{pmatrix} \rho^{S_Y}(k) + c\left(dT^{S_Y}(k) - dt^{S_Y}(k)\right) \\ +T^{S_Y}(k) + I_X^{S_Y}(k) + MP_{P,X}^{S_Y}(k) + n_{P,X}^{S_Y}(k) \\ +b_{P,X}^{S_Y}(k) \end{pmatrix} \quad (1)$$

$$\varphi_X^{S_Y}(k) = \begin{pmatrix} \rho^{S_Y}(k) + c\left(dT^{S_Y}(k) - dt^{S_Y}(k)\right) \\ +T^{S_Y}(k) - I_X^{S_Y}(k) + MP_{\varphi,X}^{S_Y}(k) + n_{\varphi,X}^{S_Y}(k) \\ +b_{\varphi,X}^{S_Y}(k) + \lambda_X A_X^{S_Y} \end{pmatrix} \quad (2)$$

where

- the superscript S_Y refers to the satellite Y,
- ρ represents the true satellite-receiver range,
- dT represents the satellite clock bias,
- dt represents the receiver clock bias,
- T represents the tropospheric delay,
- I_X represents the ionospheric delay at freq. X,
- MP_P and MP_φ represent the errors due to multipath on the code and phase pseudoranges,
- n_P and n_φ represent the error due to thermal noise on the code and phase pseudoranges,
- $b_{P,X}^{S_Y}$ and $b_{\varphi,X}^{S_Y}$ represent the satellite+receiver code and phase biases at frequency X.
- A_X represents the carrier phase ambiguity at frequency X,
- λ_X represents the wavelength of the carrier X.

In order to gather the elements of (1) and (2) that are common to the different frequencies and observables of satellite S_Y, they can be re-written as:

$$P_X^{S_Y}(k) = D^{S_Y}(k) + I_X^{S_Y}(k) + MP_{P,X}^{S_Y}(k) + n_{P,X}^{S_Y}(k) + b_{P,X}^{S_Y}(k) \quad (3)$$

$$\varphi_X^{S_Y}(k) = D^{S_Y}(k) - I_X^{S_Y}(k) + MP_{\varphi,X}^{S_Y}(k) + n_{\varphi,X}^{S_Y}(k) + b_{\varphi,X}^{S_Y}(k) + \lambda_X A_X^{S_Y} \quad (4)$$

where

$$D^{S_Y}(k) = \rho^{S_Y}(k) + c\left(dT^{S_Y}(k) - dt^{S_Y}(k)\right) + T^{S_Y}(k)$$

It is well-known that the ionospheric term can be approximated, at the first order, by:

$$I_X^{S_Y}(k) = \frac{40.3 \cdot STEC^{S_Y}(k)}{f_X^2}$$

where

- f_X is the signal's carrier frequency, and
- $STEC$ is the Slant Total Electron Content (TEC), which represents the TEC along the signal propagation path.

III. Presentation of the Ionosphere Estimation Techniques

The reference ionosphere delay estimation technique is fully presented in [2] and is only briefly described here.

A. Dual Frequency Measurements

The ionosphere delay for each visible satellite can be estimated from two signal at two frequencies using dual-frequency code geometry-free combinations as follows:

$$\kappa_{X_1,X_2}\left(P_{X_1}^{S_Y}(k) - P_{X_2}^{S_Y}(k)\right) = \begin{pmatrix} I_{X_1}^{S_Y}(k) \\ +\kappa_{X_1,X_2}\begin{pmatrix} MP_{P,X_1}^{S_Y}(k) - MP_{P,X_2}^{S_Y}(k) \\ +b_{P,X_1}^{S_Y}(k) - b_{P,X_2}^{S_Y}(k) \\ +n_{P,X_1}^{S_Y}(k) - n_{P,X_2}^{S_Y}(k) \end{pmatrix} \end{pmatrix} \quad (5)$$

with $\kappa_{X_1,X_2} = \frac{f_{X_2}^2}{f_{X_2}^2 - f_{X_1}^2}$

In the case of an E5a and E5b combination, the coefficient $\kappa_{E5b,E5a}$ is equal to 19.9 when estimating the ionospheric delay at E5a. This means that all the tracking errors (due to multipath, noise, interference) and hardware biases are multiplied by 19.9 when estimating the ionospheric delay at E5a. It is quite clear that this is very detrimental to the accuracy of the ionospheric delay estimation. It is then interesting to use dual frequency geometry-free carrier-phase combinations instead:

$$\kappa_{X_1,X_2}\left(\varphi_{X_1}^{S_Y}(k) - \varphi_{X_2}^{S_Y}(k)\right) = \begin{pmatrix} -I_{X_1}^{S_Y}(k) \\ +\kappa_{X_1,X_2}\begin{pmatrix} MP_{\varphi,X_1}^{S_Y}(k) - MP_{\varphi,X_2}^{S_Y}(k) \\ +b_{\varphi,X_1}^{S_Y}(k) - b_{\varphi,X_2}^{S_Y}(k) \\ +n_{\varphi,X_1}^{S_Y}(k) - n_{\varphi,X_2}^{S_Y}(k) \\ +\lambda_{X_1}A_{X_1}^{S_Y} - \lambda_{X_2}A_{X_2}^{S_Y} \end{pmatrix} \end{pmatrix} \quad (6)$$

In this case, the multiplication factor is not as problematic as the carrier phase tracking errors are only at the mm/cm level. However, in this case, a float ambiguity term (coming from the carrier phase ambiguities) - $\lambda_{X_1}A_{X_1}^{S_Y} - \lambda_{X_2}A_{X_2}^{S_Y}$ - has to be estimated as well. It is thus necessary to estimate the ambiguity terms together with the ionosphere term. As a consequence, the system has more unknowns than measurements.

B. Single Frequency Measurements

If only one frequency is available, the ionospheric delay of each satellite can then be estimated using the Code-Minus-Carrier (CMC) combinations as follows:

$$\frac{1}{2}\left(P_{X_1}^{S_Y}(k) - \varphi_{X_1}^{S_Y}(k)\right) \approx \begin{pmatrix} I_{X_1}^{S_Y}(k) \\ +\frac{1}{2}\begin{pmatrix} MP_{P,X_1}^{S_Y}(k) + n_{P,X_1}^{S_Y}(k) \\ +b_{P,X_1}^{S_Y}(k) - b_{\varphi,X_1}^{S_Y}(k) - \lambda_{X_1}A_{X_1}^{S_Y} \end{pmatrix} \end{pmatrix} \quad (7)$$

The above equation takes into account the fact that code tracking errors are two degrees of magnitude greater than the carrier phase tracking errors. As it can be seen, the CMC combination also integrates the carrier phase ambiguities and thus these ambiguities have to be jointly estimated with the ionosphere delay.

C. Local Ionospheric Model

To reduce the number of unknowns in the dual-frequency and single-frequency systems shown above, it is possible to try to use a simple local ionospheric delay model. This creates

another advantage which is to link the ionospheric delay terms associated with each visible satellite with a set of parameters to estimate. Modeling the local variations of the vertical ionospheric delay around the user to facilitate the estimation of the ionospheric slant delay has been used for single-frequency (GPS L1 C/A) ionospheric estimation in [8; 9] and has also been used for dual frequency GPS L1/L2 measurements in [10] in the context of Precise Point Positioning (PPP) using a network of reference stations. These models assume that the ionospheric delays can be modeled using:

- A single layer ionospheric model that is such that each point of the ionosphere layer equals the VTEC
- A local VTEC model that is such that the VTEC at any ionospheric pierce point (intersection between the assumed single-layer ionosphere and the signal propagation path) can be modeled as a function of:
  - the VTEC at a specific reference point, and
  - a VTEC gradient according to the difference in latitude and longitude between the pierce point location and the reference position.
- A mapping function that maps the VTEC at the ionosphere pierce point into the STEC. A typical mapping function to transform the VTEC into an STEC is [Lestarquit et al, 1999]:

$$MF^{S_Y}(k) = \frac{1}{\sqrt{1 - \left(\frac{R_e cos\left(E^{S_Y}(k)\right)}{R_e + h_I}\right)^2}} \qquad (8)$$

where

- R_e is the Earth radius (6378.1363 km),
- E is the satellite elevation (in rad), and
- h_I is the height of the maximum TEC, which is also the height of the ionosphere layer modeled as a single-layer.

Nine simple local VTEC models derived from the above general model were tested in [2] in the case of a Galileo E5a/E5b receiver. The elected one was based on the the expression of the VTEC at the ionosphere pierce point as a function of 5 parameters:

- The VTEC at the zenith of the user $VTEC_u$, and
- 4 VTEC gradients in the North g_N, East g_E, South g_S, West g_W directions
- The considered latitude of the ionosphere pierce point and the user location is the geomagnetic latitude.

This local VTEC model can be represented as:

$$\widehat{VTEC}_p(k) = \begin{pmatrix} VTEC_u(k) \\ +max\left(lat_p^{S_Y}(k) - lat_u(k), 0\right) \cdot g_N(k) \\ +min\left(lat_p^{S_Y}(k) - lat_u(k), 0\right) \cdot g_S(k) \\ +max\left(long_p^{S_Y}(k) - long_u(k), 0\right) \cdot g_E(k) \\ +min\left(long_p^{S_Y}(k) - long_u(k), 0\right) \cdot g_W(k) \end{pmatrix} \qquad (9)$$

where

- $lat_u \; and \; lat_p$ are the user and pierce point latitudes, and
- $long_u \; and \; long_p$ are the user and pierce point longitudes.

Using the fact that the ionospheric delay at frequency X_1 for satellite S_Y can be modeled as:

$$\hat{I}_{X_1}^{S_Y}(k) = \frac{40.3 \cdot MF^{S_Y}(k) \widehat{VTEC}_p(k)}{f_{X_1}^2}$$

It follows that:

$$\hat{I}_{X_1}^{S_Y}(k) = K_{X_1}^{S_Y}(k) \begin{pmatrix} VTEC_u(k) \\ +\max\left(\Delta lat_{u,p}^{S_Y}(k), 0\right) \cdot g_N(k) \\ +\min\left(\Delta lat_{u,p}^{S_Y}(k), 0\right) \cdot g_S(k) \\ +\max\left(\Delta long_{u,p}^{S_Y}(k), 0\right) \cdot g_E(k) \\ +\min\left(\Delta long_{u,p}^{S_Y}(k), 0\right) \cdot g_W(k) \end{pmatrix} \qquad (10)$$

where

- $K_{X_1}^{S_Y}(k) = \frac{40.3 \cdot MF^{S_Y}(k)}{f_{X_1}^2}$
- $\Delta lat_{u,p}^{S_Y}(k) = lat_p^{S_Y}(k) - lat_u(k)$
- $\Delta long_{u,p}^{S_Y}(k) = long_p^{S_Y}(k) - long_u(k)$

D. Ionosphere Estimation using Galileo E5 Only

The ionospheric delay estimation described in [2] is based on a Kalman filter that uses (1) the dual frequency code and carrier phase measurements as measurements and (2) the local VTEC model parameters and the ambiguity terms as state parameters.

The state matrix is thus:

$$\begin{bmatrix} \Delta P_{E5a,E5b}^{S_1}(k) \\ \Delta P_{E5a,E5b}^{S_2}(k) \\ \cdots \\ \Delta P_{E5a,E5b}^{S_n}(k) \\ \Delta \varphi_{E5b,E5a}^{S_1}(k) \\ \Delta \varphi_{E5b,E5a}^{S_2}(k) \\ \cdots \\ \Delta \varphi_{E5b,E5a}^{S_n}(k) \end{bmatrix} = H \begin{bmatrix} VTEC_u(k) \\ g_N(k) \\ g_S(k) \\ g_E(k) \\ g_W(k) \\ A_{E5b,E5a}^{S_1} \\ A_{E5b,E5a}^{S_2} \\ \cdots \\ A_{E5b,E5a}^{S_n} \end{bmatrix} + \begin{bmatrix} N_{P,E5a,E5b}^{S_1}(k) \\ N_{P,E5a,E5b}^{S_2}(k) \\ \cdots \\ N_{P,E5a,E5b}^{S_n}(k) \\ N_{\varphi,E5a,E5b}^{S_1}(k) \\ N_{\varphi,E5a,E5b}^{S_2}(k) \\ \cdots \\ N_{\varphi,E5a,E5b}^{S_n}(k) \end{bmatrix}$$

with

- $\Delta P_{E5a,E5b}^{S_Y} = P_{E5a}^{S_Y} - P_{E5b}^{S_Y}$
- $\Delta \varphi_{E5b,E5a}^{S_Y} = \varphi_{E5b}^{S_Y} - \varphi_{E5a}^{S_Y}$
- $A_{E5b,E5a}^{S_1} = \lambda_{E5b} A_{E5b}^{S_Y} - \lambda_{E5a} A_{E5a}^{S_Y}$
- $N_{P,E5a,E5b}^{S_1}$ and $N_{\varphi,E5a,E5b}^{S_1}$ are the observation noise assumed Gaussian.
- $H = \frac{1}{\kappa_{E5a,E5b}} \begin{bmatrix} \bar{\bar{K}}_{E5a}(k) & \overline{\overline{\Delta lat}}\ (k) & \overline{\overline{\Delta long}}\ (k) & \bar{\bar{0}}_n \\ \bar{\bar{K}}_{E5a}(k) & \overline{\overline{\Delta lat}}\ (k) & \overline{\overline{\Delta long}}\ (k) & \kappa_{E5a,E5b} \bar{\bar{I}}_n \end{bmatrix}$

where

- $\overline{\overline{\mathrm{K}}}_{\mathrm{E5a}}(\mathrm{k}) = \begin{bmatrix} \mathrm{K}_{E5a}^{\mathrm{S}_1}(\mathrm{k}) \\ \mathrm{K}_{E5a}^{\mathrm{S}_2}(\mathrm{k}) \\ \cdots \\ \mathrm{K}_{E5a}^{\mathrm{S}_n}(\mathrm{k}) \end{bmatrix}$,
- $\overline{\overline{\Delta\mathrm{lat}}}\ (\mathrm{k}) = \begin{bmatrix} \max(\Delta\mathrm{lat}_{u,p}^{\mathrm{S}_1}(\mathrm{k}),0) & \min(\Delta\mathrm{lat}_{u,p}^{\mathrm{S}_1}(\mathrm{k}),0) \\ \max(\Delta\mathrm{lat}_{u,p}^{\mathrm{S}_2}(\mathrm{k}),0) & \min(\Delta\mathrm{lat}_{u,p}^{\mathrm{S}_2}(\mathrm{k}),0) \\ \cdots & \cdots \\ \max(\Delta\mathrm{lat}_{u,p}^{\mathrm{S}_n}(\mathrm{k}),0) & \min(\Delta\mathrm{lat}_{u,p}^{\mathrm{S}_n}(\mathrm{k}),0) \end{bmatrix}$,
- $\overline{\overline{\Delta\mathrm{long}}}\ (\mathrm{k}) = \begin{bmatrix} \max(\Delta\mathrm{long}_{u,p}^{\mathrm{S}_1}(\mathrm{k}),0) & \min(\Delta\mathrm{long}_{u,p}^{\mathrm{S}_1}(\mathrm{k}),0) \\ \max(\Delta\mathrm{long}_{u,p}^{\mathrm{S}_2}(\mathrm{k}),0) & \min(\Delta\mathrm{long}_{u,p}^{\mathrm{S}_2}(\mathrm{k}),0) \\ \cdots & \cdots \\ \max(\Delta\mathrm{long}_{u,p}^{\mathrm{S}_n}(\mathrm{k}),0) & \min(\Delta\mathrm{long}_{u,p}^{\mathrm{S}_n}(\mathrm{k}),0) \end{bmatrix}$,
- $\overline{\overline{0}}_{\mathrm{n}}$ is a n-by-n zero matrix
- $\overline{\overline{\mathrm{I}}}_{\mathrm{n}}$ is a n-by-n identity matrix

It is interesting to note that this system has the advantage to separate the inter-frequency bias from the ionospheric delay terms since the inter-frequency bias will be absorbed by the (float) ambiguity state once the filter has converged.

The transition matrix is based on the following assumptions:

- The ionosphere-related terms are modeled as first-order Gauss-Markov processes.
- The ambiguity terms are modeled as first-order Gauss-Markov processes since these states will absorb the potential variation of the hardware biases as well as the ionosphere modeling error
- The Earth rotation is taken into account to update the vertical ionospheric delay between 2 consecutive time updates.

The transition matrix associated to the reference local ionosphere model is thus:

$$\begin{bmatrix} \mathrm{VTEC_u}(\mathrm{k}+1) \\ \mathrm{g_N}(\mathrm{k}+1) \\ \mathrm{g_S}(\mathrm{k}+1) \\ \mathrm{g_E}(\mathrm{k}+1) \\ \mathrm{g_W}(\mathrm{k}+1) \\ \mathrm{A}_{\mathrm{E5a,E5b}}^{\mathrm{S}_1}(\mathrm{k}+1) \\ \mathrm{A}_{\mathrm{E5a,E5b}}^{\mathrm{S}_2}(\mathrm{k}+1) \\ \cdots \\ \mathrm{A}_{\mathrm{E5a,E5b}}^{\mathrm{S}_n}(\mathrm{k}+1) \end{bmatrix} = \mathrm{F} \begin{bmatrix} \mathrm{VTEC_u}(\mathrm{k}) \\ \mathrm{g_N}(\mathrm{k}) \\ \mathrm{g_S}(\mathrm{k}) \\ \mathrm{g_E}(\mathrm{k}) \\ \mathrm{g_W}(\mathrm{k}) \\ \mathrm{A}_{\mathrm{E5a,E5b}}^{\mathrm{S}_1}(\mathrm{k}) \\ \mathrm{A}_{\mathrm{E5a,E5b}}^{\mathrm{S}_2}(\mathrm{k}) \\ \cdots \\ \mathrm{A}_{\mathrm{E5a,E5b}}^{\mathrm{S}_n}(\mathrm{k}) \end{bmatrix} + \begin{bmatrix} \sigma_{\mathrm{VTEC}} \cdot \mathrm{n_{VTEC}} \\ \sigma_{\mathrm{G_N}} \cdot \mathrm{n_{G_N}} \\ \sigma_{\mathrm{G_S}} \cdot \mathrm{n_{G_S}} \\ \sigma_{\mathrm{G_E}} \cdot \mathrm{n_{G_E}} \\ \sigma_{\mathrm{G_W}} \cdot \mathrm{n_{G_W}} \\ \sigma_{\mathrm{A}} \cdot \mathrm{n}_{\mathrm{A}^{\mathrm{S}_1}} \\ \cdots \\ \sigma_{\mathrm{A}} \cdot \mathrm{n}_{\mathrm{A}^{\mathrm{S}_n}} \end{bmatrix}$$

with

$$\mathrm{F} = \begin{bmatrix} 1 & 0 & 0 & \mathrm{W_e} & \cdots & 0 \\ 0 & 1 & 0 & 0 & \cdots & 0 \\ 0 & 0 & 1 & 0 & \cdots & 0 \\ 0 & 0 & 0 & 1 & \cdots & 0 \\ \cdots & \cdots & \cdots & \cdots & \cdots & \cdots \\ 0 & 0 & 0 & 0 & 0 & 1 \end{bmatrix}$$

where

- σ_{VTEC}, $\sigma_{\mathrm{G_N}}$, $\sigma_{\mathrm{G_S}}$, $\sigma_{\mathrm{G_E}}$, $\sigma_{\mathrm{G_W}}$, are the standard deviations associated with the variation of the local ionosphere parameters,
- σ_{A} corresponds to the standard deviation associated with the variation of the ambiguity term (mostly due to the ionosphere modeling error variation).
- $\mathrm{n_{VTEC}}$, $\mathrm{n_{G_N}}$, $\mathrm{n_{G_S}}$, $\mathrm{n_{G_E}}$, $\mathrm{n_{G_W}}$, $\mathrm{n}_{\mathrm{A}^{\mathrm{S}_1}}, \ldots, \mathrm{n}_{\mathrm{A}^{\mathrm{S}_Y}}$ are independent Gaussian noise with a unit variance, and
- $\mathrm{W_e}$ is the Earth rotation rate (rad/s)

E. Ionosphere Estimation for Galileo E5/GPS L5

When using Galileo E5 and GPS L5, the estimation process has to be amended since Galileo will provide dual-frequency measurements, while GPS will only provide measurements on L5. Using CMC measurements for GPS L5, the system to solve is now:

$$\begin{bmatrix} \Delta P_{E5a,E5b}^{S_1}(k) \\ \Delta P_{E5a,E5b}^{S_2}(k) \\ \cdots \\ \Delta P_{E5a,E5b}^{S_n}(k) \\ \Delta\varphi_{E5b,E5a}^{S_1}(k) \\ \Delta\varphi_{E5b,E5a}^{S_2}(k) \\ \cdots \\ \Delta\varphi_{E5b,E5a}^{S_n}(k) \\ CMC_{L5}^{S_1'}(k) \\ CMC_{L5}^{S_2'}(k) \\ \cdots \\ CMC_{L5}^{S_m'}(k) \end{bmatrix} = H \begin{bmatrix} VTEC_u(k) \\ g_N(k) \\ g_S(k) \\ g_E(k) \\ g_W(k) \\ A_{E5b,E5a}^{S_1} \\ A_{E5b,E5a}^{S_2} \\ \cdots \\ A_{E5b,E5a}^{S_n} \\ A_{L5}^{S_1'} \\ A_{L5}^{S_2'} \\ \cdots \\ A_{L5}^{S_m'} \end{bmatrix} + \begin{bmatrix} N_{P,E5a,E5b}^{S_1}(k) \\ N_{P,E5a,E5b}^{S_2}(k) \\ \cdots \\ N_{P,E5a,E5b}^{S_n}(k) \\ N_{\varphi,E5a,E5b}^{S_1}(k) \\ N_{\varphi,E5a,E5b}^{S_2}(k) \\ \cdots \\ N_{\varphi,E5a,E5b}^{S_n}(k) \\ N_{CMC,L5}^{S_1'}(k) \\ N_{CMC,L5}^{S_2'}(k) \\ \cdots \\ N_{CMC,L5}^{S_m'}(k) \end{bmatrix}$$

As it is easy to have the expression of the matricx H from this system from what was presented in the Galileo E5 only case, this will not be detailed here. The same deduction can be done regarding the transition matrix F.

F. Ionosphere Estimation for Dual Constellation / Dual Frequency

For references, a third test case was investigated. This test case aimed at assessing the performance of the estimation process in the case of Galileo E5 together with another constellation that would have two available signals in the E5 band. This case is interesting as it would allow using dual frequency carrier phase measurements instead of CMC, which are much noisier. As a consequence, a 'fictitious' GPS constellation was used that assumed that GPS satellites were able to transmit an ALTBOC(15,10) on the same frequency as Galileo E5. By doing so, the idea was to test the estimation process using dual constellation dual frequency carrier phase measurements.

As in the case of Galileo E5/GPS L5, the Kalman filter equations can be deduced from what was presented in the Galileo E5 only case as the local VTEC model is assumed the same.

G. Local VTEC Model based on 3 Gradients

In [2], the true VTEC variations from obtained from the NeQuick model were analyzed. It was observed that there could be some potential strong variations of the gradients in the North/South directions over Europe. This is why it was decided in the first place to have separate North and South gradients.

However, the variation in the East/West direction appeared more linear. As a consequence, in the frame of this paper, another local VTEC model will be tested based on only 3 gradients: North, South and East/West. The will to test this model is to see how a model with less parameters would behave, in particular taking advantage of a greater observability of each parameter.

IV. Presentation of the Simulation Tool and Filter Settings

A. Simulation Tool

The simulation tool is exactly the same as the one used in [2]. There are however two differences:

- the true ionosphere is now modeled using the NeQuick2 model, an evolution of the NeQuick model freely available on the ITU website and used in [12; 13; 14]. For visualization purposes, the C/N_0 for the considered Galileo E5 signals's component at the user antenna output is shown in Figure 1**Erreur ! Source du renvoi introuvable.**. The difference between NeQuick1 and NeQuick2 is mainly that the variation of the VTEC are not as sharp in NeQuick2 as it is in NeQuick1 due to modifications in the modeling of the high altitude ionosphere layers.
- GPS satellites are assumed to follow the GPS constellation defined in [4]. The link budget associated with the GPS satellites takes into account the power output difference between GPS and Galileo signals.
- Multipath are generated assuming single reflector (the Earth surface) and the user antenna located on a pole 2 meters above the ground.

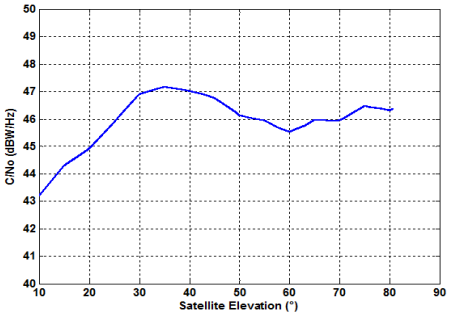

Figure 1 – C/N_0 of Galileo E5a Signals at the Antenna Output

B. Kalman Filter Settings

The observation noise variance was chosen to be the product of a C/N_0-dependent term and an elevation-dependent term. The C/N_0-dependent term is the usual theoretical tracking noise variance [11]. The elevation-dependent variance represents the impact of multipath and was chosen to be equal to $\frac{1}{4}\left(3+\frac{1}{\sin\left(E^{S}Y(k)\right)}\right)$.

The chosen covariance matrix for the process noise was set empirically to allow for a variation of 0.1 cm/s for the vertical ionosphere component, 0.5 cm/rad/s for the gradients, and 0.01cm/s for the ambiguity terms.

C. Simulation Parameters

The receiver mask was chosen equal to 10°.

Five locations were selected to represent a diversity in terms of latitudes and longitudes:

- **Sevilla**, which is supposed to be close to the VTEC peak and should thus have higher VTEC gradients
- **Toulouse**, which is in the middle of Europe (in terms of latitude) and should have average VTEC gradients, and
- **Stockholm**, which is in the upper part of Europe (in terms of latitude) and should have low VTEC gradients
- **Beijing**, which sees an ionosphere activity that should be similar to Sevilla (see Figure 2)
- **Shanghai,** which is very close to the VTEC peak and can be considered as a worst case scenario (see Figure 2).

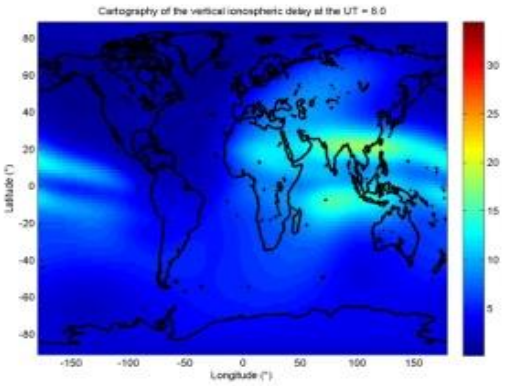

Figure 2 – Representation of the VTEC with the VTEC Peak Located over Southern Asia

Also, four time periods were used to represent the TEC during a plurality of ionosphere activities. These periods were selected thanks to the table of the monthly R12 indexes over the period 1931-2001 provided by ITU (its cumulative distribution is shown in Figure 3) [12]. The four periods selected were:

- **May 1958,** it has a R12 value representing an extremely active ionosphere (99% of all the R12 values in the ITU table are lower)
- **May 1980** it has a R12 value representing a very active ionosphere (95% of all the R12 values in the ITU table are lower)
- **Sept. 2002** it has a R12 value representing an active ionosphere (66% of all the R12 values in the ITU table are lower)
- **July 1998** it has a R12 value representing an median ionosphere activity (50% of all the R12 values in the ITU table are lower)

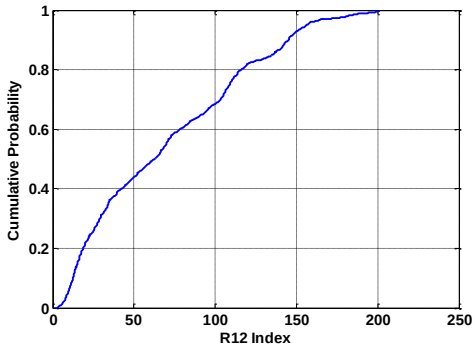

Figure 3 – Cumulative Distribution of Monthly R12 indexes

V. SIMULATION RESULTS

A. Analysis of Results in Europe

The simulations were then run for the 5 locations, for the 4 time slots, and for all the configurations (Galileo E5 only, Galileo E5/GPS L5, Galileo E5/'fictitious GPS dual frequency').

Four output of the simulations are analyzed:

- the max ionosphere estimation error at L1,
- the 68th percentile of the ionosphere estimation error at L1
- the 95th percentile of the ionosphere estimation error at L1
- the 99th percentile of the ionosphere estimation error at L1

The ionosphere estimation errors are given at L1 since this is the usual reference frequency at the moment. In the following, the statistics are computed considering only the ionosphere estimation error of:

- all Galileo satellites above the receiver mask (10°) and
- all Galileo satellites above 30°, still considering that all satellites above 10° are use.

The results for the European cities of the simulations are provided in Table 1 for satellites above 10°, and in Table 2 for the satellites above 30° (Table 2 also only presents the results for the 4-gradient local VTEC model). In these tables, the lowest values for a given day and location are in bold.

It appears generally that the best results are obtained when using dual constellation with dual-frequency. The main advantage of this configuration over the Galileo E5 only configuration is to limit the occurrence of large errors as seen with the maximum and 99th percentile of the ionosphere estimation error. This is true mostly in the difficult cases (very high ionosphere activity). This means that the use of the dual constellation dual frequency case allows a better assessment of the rising and setting satellites' ionosphere delay, probably due to the fact that twice as many satellites are used and that the ionosphere sounding is thus more distributed around the user. However, for a quieter ionosphere, the results between the dual constellation dual frequency and single constellation dual frequency are quite comparable. The main reason is that the main source of error of the proposed ionosphere estimation process in a quieter situation is the chosen model itself: the local VTEC model itself as well as the mapping function.

The dual constellation dual frequency configuration allows having worst case ionosphere estimation error below 2 meters and a standard deviation of the ionosphere estimation error below 30 cm in the 3 European cities. When looking only at satellites above 30° (see Table 2), these worst case results show a maximum error below 1 m and a standard deviation of the estimation error below 20 cm in the 3 European cities. This is an excellent result considering that these results include the top 1% of the strongest ionosphere activity.

Finally, the Galileo E5/GPS L5 configuration appears to provide the worst results. This is even quite significant for simulations in Toulouse and Sevilla where the ionosphere is more active. The main reason that the GPS L5 CMC measurements are much more affected by multipath than Galileo E5a/E5b dual frequency carrier-phase measurements. This can create local errors that leak into the ionosphere parameters resulting in large estimation errors, particular for low elevation satellites

From Table 1, it can also be seen that the choice of 3 or 4 gradients does not make much of a difference in the estimation process. Thus validating that the VTEC is almost linear in the East/West direction.

B. Detailed Analysis of Results for Toulouse in May 1980

In order to understand the estimation process, a specific analysis of a test case is interesting. The test case chosen here is the case of Toulouse in May 1980. The number of visible Galileo and GPS satellites over a day is shown in Figure 4.

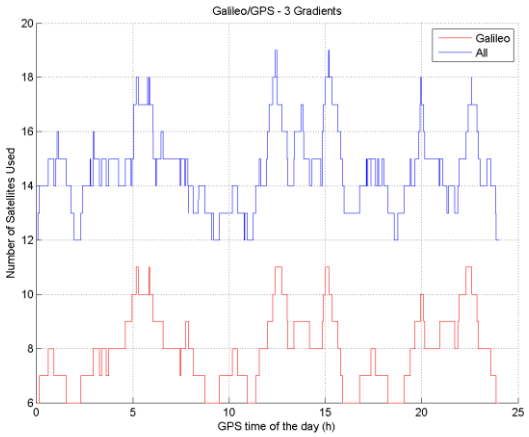

Figure 4 – Number of Visible Satellites (above 10°) in Toulouse in the Considered Scenario

In the dual constellation dual frequency configuration, Figure 5 and Figure 6 show the output of the estimation process (vertical ionosphere and gradients respectively). The observation of the estimated gradient show that while the estimated North and South gradients can differ quite significantly, thus justifying the use of 2 different parameters, this is not the case of the East and West gradients that tend to remain with the same value. This explains that the cases of 3 and 4 gradients in the estimation process do not lead to significantly different results.

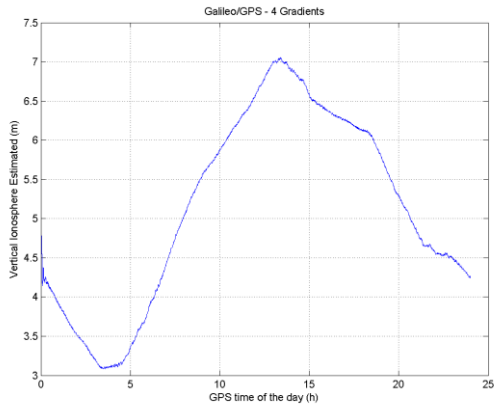

Figure 5 – Estimated Vertical Ionosphere based on Two Dual Frequency (in E5) Constellations in Toulouse in May 1980

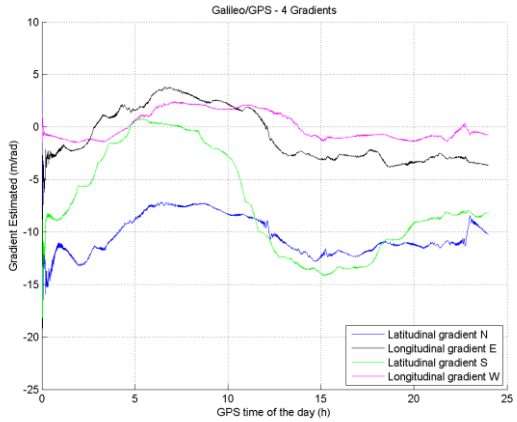

Figure 6 – Estimated Gradients based on Two Dual Frequency (in E5) Constellations in Toulouse in May 1980 conditions

Figure 7 represents the actual ionosphere estimation error at L1 for the Galileo satellites. It can be seen that the major errors are coming from rising and setting satellites, while when the satellite is at medium to high elevation, the estimation error is almost systematically below 0.5 meter.

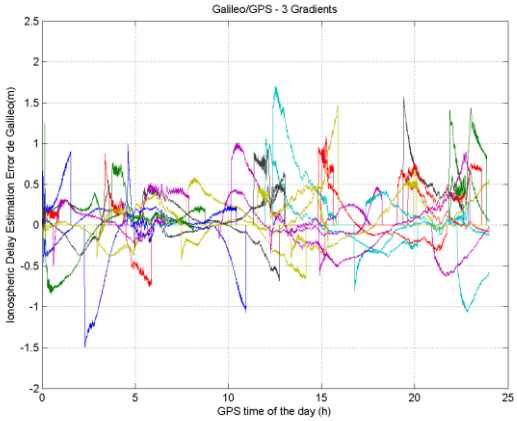

Figure 7 – Ionosphere Estimation Error (at L1) based on Two Dual Frequency (in E5) Constellations in Toulouse in May 1980 conditions

Figure 8 and Figure 9 show the ionosphere delay error as a function of the ionosphere pierce point longitude and geomagnetic latitude with respect to the user location (respectively). It can be seen that the highest uncertainty seem to come on the latitude (North/South) since the plots create a wide area. On the other hand, in the East/West direction (longitude), a trend seem to appear as a second order function in which the ionosphere error seems to grow when the difference between the longitude of the pierce point and of the user increases. This could mean that a more optimal local VTEC could be found.

Other local VTEC were tested to take into account this observation, in particular by adding a second order coefficient for the gradients. However, no improvement was noticeable in other tested configurations. It is believed that the use of a more optimal local VTEC model might only bring marginal improvement since there is also an uncertainty on the actual accuracy of the mapping function when the ionosphere is very active.

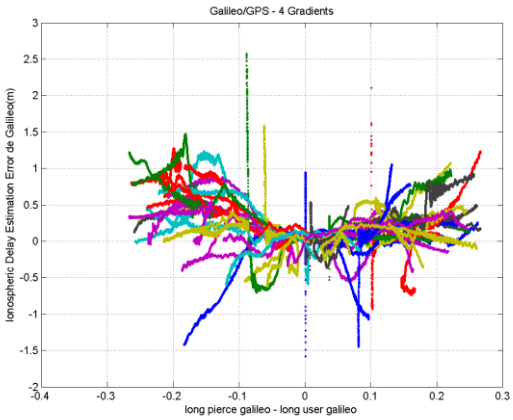

Figure 8 – Ionosphere Estimation Error (at L1) as a Function of the Pierce Point Longitude based on Two Dual Frequency (in E5) Constellations in Toulouse in May 1980 conditions

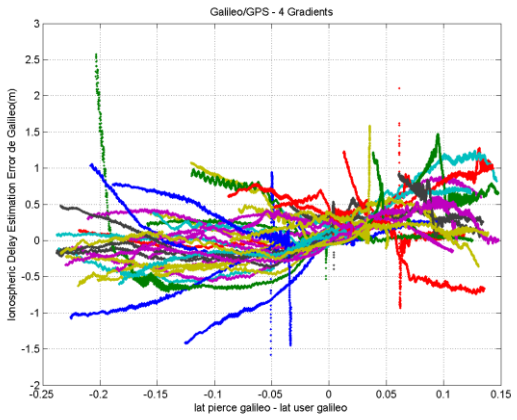

Figure 9 – Ionosphere Estimation Error (at L1) as a Function of the Pierce Point Latitude based on Two Dual Frequency (in E5) Constellations in Toulouse in May 1980 conditions

C. Analysis of Results in Asia

Table 3 and Table 4 show the results for Beijing and Shanghai only for the dual frequency cases and only for the 4-gradient local VTEC model. It can be seen that the results in Beijing are similar to the ones in Europe, which is not surprising as it has a similar geomagnetic latitude.

However, Shanghai shows very large estimation errors with worst case situations reaching almost 5m (above 60cm standard deviation). This is due to the difficulty for the proposed linear VTEC model to accommodate the vicinity of the VTEC peak that creates large non-linear variations. Still the results can be seen as reasonable given the conditions.

VI. CONCLUSIONS

This paper has shown further results to the ionosphere delay estimation process that was presented in [1], [15] and [2]. In particular, it is based on a more representative ionosphere condition due to the use of the latest NeQuick model for the simulations. It also proposed the use of a new local VTEC model and of new receiver configurations.

The simulation results show that the proposed ionosphere estimation process, when having access only to the E5 band and to two constellations with two frequencies in the band, can be quite interesting in Europe even in case of a very active ionosphere. Indeed, it was shown that in one of the worst case situations (top 1% of the greatest ionosphere activity), the standard deviation of the ionosphere estimation error at L1 was below 30 cm for satellites above 10° and below 20cm for satellites above 30°. It also showed that the maximum error was around 2m (and below 1m 99% of the time).

It was also shown that it was very interesting even if only one dual frequency constellation (Galileo) was available in the E5 band as a significant performance degradation with respect to the dual constellation configuration was only seen for extremely active ionosphere conditions.

Finally, the use of a second constellation with only one signal in the E5 band was shown not to be very interesting as it increased the estimation error due to the use of CMC measurements.

The limitation of the model was also highlighted when the user location becomes too close to the VTEC peak location as the simple linear local model then cannot accommodate large and steep VTEC variations in several directions.

REFERENCES

[1] Julien O., Macabiau C., Issler J-L., L. Lestarquit, *Ionospheric Delay Estimation Strategies Using Galileo E5 Signals Only*, Proceedings of the ION GNSS 2009, Savannah, GA, USA

[2] Julien O., Issler J-L., L. Lestarquit, *Ionospheric Delay Estimation Using Galileo E5 Signals Only*, Proceedings of the ION GNSS 2012, Nashville, TN, USA

[3] European Union, European GNSS (Galileo) Open Service Signal-in-Space Interface Control Document.

[4] RTCA SC-159, Assessment of Radio Frequency Interference Relevant to the GNSS L5/E5a Frequency Band, RTCA DO 292, July 2004.

[5] Bastide, F.: Analysis of the Feasibility and Interests of Galileo E5a/E5b and GPS L5 Signals for Use with Civil Aviation, PhD. Thesis, 2004.

[6] Lestarquit, L., G. Artaud, J-L Issler (2008), ALTBOC for Dummies or Everything you Always wanted to Know about ALTBOC, Proceedings of the ION GNSS 2008.

[7] Simski, A, J.-M. Sleewaegen, M. Hollreiser, and M. Crisci (2006), Performance Assessment of Galileo Ranging Signals Transmitted by GSTB-V2 Satellites, Proceedings of the 1992 Institute Of Navigation GPS Conference (Albuquerque, NM, Sept. 16-18), pp. 483-490.

[8] Lestarquit, L. N. Suard, and J.-L. Issler, Determination of the Ionospheric Error using only L1 Frequency GPS Receiver, Proceedings of the 1997 ION National Technical Meeting (Santa Monica, CA, Jan 14-16), pp. 313-322.

[9] Moreno, R., N. Suard, Ionospheric delay using only L1: validation and application to GPS receiver calibration and to inter-frequency biases estimation, Proceedings of the 1999 ION National Technical Meeting (San Diego, CA, Jan. 25-27), pp. 119-125.

[10] Komjathy A, Global ionospheric Total Electron Content mapping using the Global Positioning System. Departments of Geodesy and Geomatics Engineering, University of New Brunswick. Fredericton, New Brunswick, Canada : s.n., 1997. Ph.D. dissertation.

[11] Van Dierendonck A.J., GPS Receivers in Global Positioning System: Theory and Practice, B. Parkinson and JJ Spilker Jr, Ed, Washington DC, AIAA, Inv, 1996

[12] ITU-R, Reference ionosphere characteristics, Recommendation P.1239. (approved in 1997-05, managed by ITU-R Study Group SG3).

[13] Radicella, S.M. and M.L. Zhang (1995), The improved DGR analytical model of electron density height profile and total electron content in the ionosphere, Annals of Geophysics., Vol 38, No. 1.

[14] Leitinger, R., Zhang, M.L., Radicella, S.M., 2005. An improved bottomside for the ionospheric electron density model NeQuick, Annals of Geophysics 48 (3), 525–534.

[15] Sahmoudi et al, U-SBAS: A Universal multi-SBAS Standard to ensure Compatibility, Interoperability and Interchangeability. NAVITEC conference. December 2010, Noordwijck.

Table 1 - Performance Analysis of the Ionospheric Delay Estimation Process in European Cities using the 6 Test Cases (Galileo Only, Galileo/GPS, Galileo/Fictitious GPS in the case of 3 and 4 gradients for the local VTEC model)

		Stockholm				Toulouse				Seville			
		1958	**1980**	**2002**	**1998**	**1958**	**1980**	**2002**	**1998**	**1958**	**1980**	**2002**	**1998**
Galileo E5 Only 4 Grad.	68th perc.	0.25	0.24	0.18	0.12	0.25	0.26	0.16	0.11	0.33	0.31	0.21	0.14
	95th perc.	0.68	0.64	0.57	0.37	**0.69**	**0.70**	**0.44**	0.32	**0.82**	0.81	0.59	**0.43**
	99th perc.	1.01	0.93	1.10	0.74	**0.97**	1.18	0.76	0.58	1.31	**1.08**	0.89	0.66
	Max	2.57	1.47	2.41	1.21	1.82	1.71	1.23	1.33	2.53	2.52	2.18	1.17
Galileo E5 Only 3 Grad.	68th perc.	0.26	0.24	0.18	0.12	0.27	0.27	0.17	0.12	0.36	0.35	0.20	0.14
	95th perc.	0.70	0.65	0.57	0.37	0.77	0.81	**0.43**	0.3	1.00	1.01	0.66	0.48
	99th perc.	1.02	0.94	0.98	0.63	1.02	1.14	0.69	0.53	1.49	1.39	1.03	0.66
	Max	2.28	1.55	2.10	1.19	1.68	1.54	**1.12**	1.23	2.84	2.84	1.65	1.15
Galileo E5 / GPS L5 4 Grad.	68th perc.	0.21	0.27	0.19	0.09	0.53	0.53	0.23	0.17	0.67	0.66	0.22	0.26
	95th perc.	**0.59**	0.77	0.49	**0.34**	1.69	1.68	0.73	0.54	1.79	1.80	0.95	0.82
	99th perc.	0.89	1.32	**0.74**	0.54	2.58	2.55	1.28	1.03	2.83	2.96	2.26	1.44
	Max	2.18	2.34	**1.19**	0.93	3.42	3.42	3.03	1.74	4.67	4.55	3.62	2.37
Galileo E5 / GPS L5 3 Grad.	68th perc.	0.20	0.28	0.18	0.11	0.58	0.59	0.26	0.16	0.79	0.76	0.24	0.28
	95th perc.	**0.66**	0.64	0.53	**0.30**	1.84	1.88	0.74	0.55	1.93	1.91	0.86	0.93
	99th perc.	1.03	1.14	**0.77**	**0.45**	2.80	2.89	1.20	1.09	2.68	3.14	1.84	1.40
	Max	1.65	1.69	1.46	0.70	3.67	4.21	2.81	1.76	5.67	5.90	3.75	2.76
Galileo E5 / GPS «Bi-Freq» 4 Grad.	68th perc.	0.25	0.24	0.17	0.10	0.26	0.27	0.14	0.11	0.31	0.32	0.19	0.13
	95th perc.	**0.62**	**0.56**	0.47	**0.28**	**0.72**	**0.70**	**0.41**	0.29	**0.78**	0.78	**0.51**	**0.38**
	99th perc.	**0.89**	**0.77**	**0.78**	**0.48**	**0.96**	**1.04**	**0.65**	0.54	**1.18**	**1.11**	**0.77**	**0.55**
	Max	**1.45**	1.29	1.25	0.73	**1.55**	**1.47**	1.15	1.19	1.90	1.93	1.48	1.16
Galileo E5 / GPS «Bi-Freq» 3 Grad.	68th perc.	0.26	0.24	0.17	0.10	0.29	0.30	0.15	0.11	0.32	0.34	0.17	0.13
	95th perc.	**0.65**	**0.58**	0.50	**0.29**	0.77	0.76	**0.42**	0.29	0.93	0.92	0.59	**0.38**
	99th perc.	**0.89**	**0.81**	**0.76**	**0.44**	1.14	1.21	**0.61**	0.52	1.28	1.27	**0.79**	**0.56**
	Max	**1.42**	**1.21**	**1.18**	**0.63**	1.63	1.70	**1.08**	1.14	**1.82**	**1.78**	**1.34**	**1.09**

Table 2 - Performance Analysis of the Ionospheric Delay Estimation Process in European Cities using the 3 Test Cases (Galileo Only, Galileo/GPS, Galileo/Fictitious GPS in the case of 4 gradients for the local VTEC model)

		Stockholm				Toulouse				Seville			
		1958	**1980**	**2002**	**1998**	**1958**	**1980**	**2002**	**1998**	**1958**	**1980**	**2002**	**1998**
Galileo E5 Only 4 Grad.	68th perc.	0.14	0.14	0.10	0.07	0.15	0.15	0.10	0.08	0.19	0.19	0.12	0.09
	95th perc.	0.36	0.33	0.24	0.18	0.38	0.37	0.23	0.18	0.48	0.49	0.30	0.22
	99th perc.	0.50	0.47	0.33	0.26	0.50	0.51	0.32	0.28	0.70	0.68	0.43	0.30
	Max	0.73	0.70	0.57	0.39	0.68	0.67	0.39	0.48	0.80	0.84	0.61	0.43
Galileo E5 / GPS L5 4 Grad.	68th perc.	0.18	0.20	0.14	0.04	0.34	0.34	0.16	0.11	0.48	0.46	0.17	0.20
	95th perc.	0.40	0.42	0.33	0.13	0.90	0.90	0.37	0.28	1.01	0.96	0.47	0.40
	99th perc.	0.57	0.57	0.51	0.21	1.40	1.39	0.50	0.43	1.45	1.42	0.70	0.59
	Max	0.75	0.75	0.58	0.33	1.66	1.63	0.99	0.63	2.22	2.16	1.54	0.94
Galileo E5 / GPS «Bi-Freq» 4 Grad.	68th perc.	0.14	0.13	0.10	0.07	0.17	0.18	0.10	0.07	0.21	0.21	0.10	0.08
	95th perc.	0.37	0.35	0.24	0.15	0.39	0.40	0.20	0.16	0.50	0.51	0.27	0.21
	99th perc.	0.54	0.50	0.33	0.21	0.54	0.53	0.30	0.27	0.71	0.67	0.38	0.30
	Max	0.73	0.70	0.57	0.28	0.71	0.66	0.40	0.43	1.03	0.98	0.49	0.46

Table 3 - Performance Analysis of the Ionospheric Delay Estimation Process in European Cities using the 6 Test Cases (Galileo Only, Galileo/GPS, Galileo/Fictitious GPS in the case of 3 and 4 gradients for the local VTEC model)

		Beijing				Shanghai			
		1958	**1980**	**2002**	**1998**	**1958**	**1980**	**2002**	**1998**
Galileo E5 Only 4 Grad.	68^{th} perc.	0.35	0.33	0.19	0.14	0.62	0.63	0.40	0.22
	95^{th} perc.	0.91	0.89	0.55	0.39	**1.75**	**1.75**	**1.10**	0.68
	99^{th} perc.	1.30	1.42	0.78	0.69	**2.64**	2.60	1.80	1.09
	Max	2.59	2.68	1.32	1.49	4.37	4.48	2.80	1.97
Galileo E5 / GPS «Bi-Freq» 4 Grad.	68^{th} perc.	0.29	0.30	0.15	0.13	0.60	0.61	0.38	0.20
	95^{th} perc.	**0.81**	**0.80**	0.44	**0.35**	**1.77**	**1.77**	**1.18**	0.64
	99^{th} perc.	**1.08**	**1.09**	**0.62**	**0.53**	**2.84**	**2.84**	**2.05**	1.23
	Max	1.76	2.07	0.92	0.95	**4.43**	**4.31**	2.63	1.94

Table 4 - Performance Analysis of the Ionospheric Delay Estimation Process in European Cities using the 3 Test Cases (Galileo Only, Galileo/GPS, Galileo/Fictitious GPS in the case of 4 gradients for the local VTEC model)

		Beijing				Shanghai			
		1958	**1980**	**2002**	**1998**	**1958**	**1980**	**2002**	**1998**
Galileo E5 Only 4 Grad.	68^{th} perc.	0.20	0.18	0.10	0.08	0.39	0.39	0.26	0.12
	95^{th} perc.	0.50	0.48	0.26	0.19	1.10	1.02	0.69	0.39
	99^{th} perc.	0.63	0.59	0.37	0.28	1.61	1.60	1.09	0.60
	Max	0.83	0.81	0.57	0.45	2.77	2.69	1.67	0.89
Galileo E5 / GPS «Bi-Freq» 4 Grad.	68^{th} perc.	0.20	0.19	0.10	0.08	0.38	0.38	0.24	0.12
	95^{th} perc.	0.49	0.48	0.23	0.17	1.12	1.04	0.72	0.40
	99^{th} perc.	0.63	0.60	0.32	0.25	1.77	1.73	1.29	0.68
	Max	0.73	0.74	0.40	0.37	2.81	2.73	1.63	0.98